

# Intraparticle Diffusion of Phosphates in OH-Type Strongly Basic Ion Exchanger

Wilmer A. Galinada and Hiroyuki Yoshida

Dept. of Chemical Engineering, Osaka Prefecture University, Sakai 599-8531, Japan

DOI 10.1002/aic.10261

Published online in Wiley InterScience (www.interscience.wiley.com).

*The intraparticle diffusions of  $H_3PO_4$ ,  $H_2PO_4^-$ ,  $HPO_4^{2-}$ , and  $PO_4^{3-}$  ions in an OH-type strongly basic ion exchanger, DIAION SA10A, were investigated by measuring the uptake curves for adsorption of phosphates by using the shallow-bed method. The experimental uptake data were correlated by applying the homogeneous Fickian diffusion model and the parallel diffusion model for surface and pore diffusions. In all phosphate systems, the values of intraparticle effective diffusivity ( $D_{eff}$ ) obtained from the homogeneous model increased with the increase in the bulk-phase concentration, and suggested the existence of a parallel transport of phosphates in the particle by the surface and pore diffusions. The surface diffusivities ( $D_s$ ) for the parallel diffusion model were determined from the intercepts of the plots of  $D_{eff}[1 + (\epsilon_P C_0/q_0)]$  vs.  $\epsilon_P C_0/q_0$ . The accurate pore diffusivities ( $D_p$ ) were obtained by matching the theoretical uptake curves for the parallel diffusion model with the experimental uptake data. The parallel diffusion model agrees reasonably well with the experimental uptake data. © 2004 American Institute of Chemical Engineers AIChE J, 50: 2806–2815, 2004*

*Keywords: phosphates, ion exchange, mass transfer, parallel diffusion, pore diffusion, surface diffusion*

## Introduction

There are several previous studies on ion-exchange rates that describe different mass transfer models. Yoshida et al. (1985) derived a theoretical equation for an intraparticle effective diffusivity in a bidispersed porous ion exchanger under the assumption of a parallel diffusion through the solid phase and the macropore. They measured the intraparticle effective diffusivity of several ions by isotopic ion exchange. They concluded that the equations for estimating the surface diffusivity in a porous-type resin were quite similar to those for gel-type resins. They also studied an intraparticle mass transfer in a bidispersed porous ion exchanger by mutual ion exchange (Yoshida and Kataoka, 1985). To prove a parallel transport of surface and pore diffusions, extensive studies on the mass transport of various direct dyes through porous cellulose mem-

branes were previously conducted (Gutsche and Yoshida, 1994; Maekawa et al., 1989; Nango et al., 1989; Yoshida et al., 1986, 1989, 1991). They measured not only uptake curves but also concentration profiles and theoretically proved the existence of a parallel transport by using the experimental uptake curves and concentration profiles. The parallel transport of BSA by surface and pore diffusions with a Langmuir-type isotherm in a highly porous and strongly basic chitosan ion exchangers was also previously reported (Yoshida et al., 1994).

Several studies on adsorption and kinetics of strong and weak acids in aqueous solutions using weak-base resins have been extensively reported (Bhandari et al., 1992a,b, 1993, 1997; Helfferich and Hwang, 1985; Rao and Gupta, 1982; Takatsuji and Yoshida, 2001; Yoshida and Takatsuji, 2000). Yoshida and Takatsuji (2000, 2001) investigated a parallel transport by surface and macropore diffusions of acetic acid and lactic acid in DIAION WA30 and Chitopearl CCS. They applied a parallel diffusion model in analyzing their experimental uptake data. In the adsorption of phosphoric acid, which is a weak polybasic acid with three dissociation equilibria on

Correspondence concerning this article should be addressed to W. A. Galinada at wilmer@novell.chem.utk.edu.

weak base resins, Bhandari et al. (1997) assumed that the contribution of the second and third dissociations was negligible in the whole range of phosphate concentrations considered. They concluded that phosphoric acid follows a dual-site adsorption mechanism similar to that observed with sulfuric acid, a strong dibasic acid. Rao and Gupta (1982) presented a study on the kinetics of ion exchange accompanied by neutralization reactions in a weak-base macroporous anion-exchange resin and showed that, even in very dilute solutions, the adsorption rate of sulfuric acid was controlled by the resin phase or pore diffusion. On the other hand, Helfferich and Hwang (1985) attempted to explain the high rate of adsorption of  $\text{H}_2\text{SO}_4$  on the basis of a "proton transfer mechanism" by diffusion of  $\text{HSO}_4^-$  ions in the resin pores.

It is apparent that the intraparticle diffusion models described in the preceding studies were mostly applied to adsorption and ion-exchange kinetics of strong and weak acids on weak-base resins. Application of these existing models to mass transfers of strong or weak acids using strong-base resins has thus far received much less attention. The scarcity of literature on this aspect is probably attributable to the fact that, in the case of polybasic acids, the adsorption behavior is much more complicated compared to that of monobasic or dibasic acids because of multiple dissociation equilibria and the difficulty in describing the adsorption equilibria and kinetics of polyvalent ions.

Recently, we reported the equilibria for adsorption of four different types of phosphate species:  $\text{H}_3\text{PO}_4$ ,  $\text{H}_2\text{PO}_4^-$ ,  $\text{HPO}_4^{2-}$ , and  $\text{PO}_4^{3-}$  on an OH-type, strongly basic anion exchanger, DIAION SA10A, in aqueous media and in wide pH ranges by the batch method (Yoshida and Galinada, 2000, 2002). We concluded that the adsorption process was technically feasible. For all phosphate systems considered, the amount of phosphate adsorption on DIAION SA10A was relatively high, and different behaviors in the adsorption isotherms for different phosphate species were observed. These peculiar behaviors were greatly influenced by the pH of the equilibrated solutions. Then by applying the mass action law to the various dissociation reactions of phosphates in the liquid-phase and ion-exchange reactions involved in the resin phase, theoretical equations for the adsorption isotherms were derived. The proposed equilibrium models were well able to correlate the experimental data and explained the peculiarities in experimental adsorption isotherms. Therefore, it is necessary to further deeply understand the intraparticle mass transport of these phosphate species in this type of ion exchanger.

In this experimental study, the intraparticle diffusions of four types of phosphate species— $\text{H}_3\text{PO}_4$ ,  $\text{H}_2\text{PO}_4^-$ ,  $\text{HPO}_4^{2-}$ , and  $\text{PO}_4^{3-}$  ions—in an OH-type, strongly basic anion exchanger, DIAION SA10A, are investigated. The experimental uptake curves for adsorption of phosphates are measured by using the shallow-bed method. The uptake data are then analyzed to elucidate the intraparticle mass transport of phosphates in the particle. The intraparticle effective diffusivities are calculated based on the homogeneous Fickian diffusion model, and the existence of a parallel transport of phosphates by surface and pore diffusions is determined. The diffusivity ratio of pore diffusivity to diffusivity in an infinitely dilute aqueous solution is also determined to further explain the intraparticle diffusion of the individual phosphate species in the liquid phase of the network of the resin and on the functional group of the resin.

## Theory

### Intraparticle diffusion based on parallel diffusion model

An intraparticle diffusion model based on a parallel diffusion for gel-type resins, developed and presented by Yoshida et al. (1991, 1994), was applied in this experimental study. The surface component of gel-type resins is continuous and a macropore, having a complicated shape, exists. Because DIAION SA10A is a gel-type resin with quaternary ammonium (type I) as a fixed functional group, the uptake of phosphate ions on the functional group and in the liquid phase inside the network structure of the resin particle proceeds by ion-exchange interaction between the strongly basic  $\text{OH}^-$  and the phosphate ions through a neutralization reaction process. In this experimental study, the intraparticle diffusion of phosphate ions in DIAION SA10A was analyzed based on a parallel transport by phosphate ion hopping from one functional group to the next functional group (hereafter called surface diffusion) and the liquid-phase diffusion inside the network structure of the resin particle (hereafter called pore diffusion). The following assumptions apply:

- (1) Surface and pore diffusions occur in parallel inside the DIAION SA10A particle.
- (2) Surface and pore diffusivities are constant throughout the adsorption process.
- (3) The diameter of the network and the void fraction of DIAION SA10A particle are constant throughout the adsorption process.
- (4) The liquid-phase concentration of phosphate ions inside the particle is in local equilibrium with the concentration of the adsorbed phosphate ions on the surface of the particle.
- (5) The bulk-phase concentration of phosphates is constant throughout the adsorption process.

The preceding assumptions then lead to a mass balance equation given by the following equation

$$\varepsilon_p \frac{\partial C}{\partial t} + \frac{\partial q}{\partial t} = D_p \varepsilon_p \frac{1}{r^2} \frac{\partial}{\partial r} \left( r^2 \frac{\partial C}{\partial r} \right) + D_s \frac{1}{r^2} \frac{\partial}{\partial r} \left( r^2 \frac{\partial q}{\partial r} \right) \quad (1)$$

where  $C$  ( $\text{mol m}^{-3}$ ) and  $q$  ( $\text{mol m}^{-3}$  wet resin) are the liquid-phase concentration of phosphate ions inside the particle and the resin-phase concentration of phosphate ions on the surface of the particle, respectively;  $\varepsilon_p$  is the void fraction of the pore; and  $D_p$  and  $D_s$  ( $\text{m}^2 \text{s}^{-1}$ ) are the pore and surface diffusivities, respectively. Using dimensionless variables, Eq. 1 is transformed into Eq. 2

$$\frac{\partial X}{\partial \tau_p} + \alpha \frac{\partial Y}{\partial \tau_p} = \frac{1}{\rho^2} \frac{\partial}{\partial \rho} \left( \rho^2 \frac{\partial X}{\partial \rho} \right) + \beta \frac{1}{\rho^2} \frac{\partial}{\partial \rho} \left( \rho^2 \frac{\partial Y}{\partial \rho} \right) \quad (2)$$

where  $X = C/C_0$ ,  $Y = q/q_0$ ,  $\tau_p = D_p t/r_0^2$ ,  $\rho = r/r_0$ ,  $\alpha = q_0/\varepsilon_p C_0$ ,  $\beta = \alpha(D_s/D_p)$ , and  $q_0$  ( $\text{mol m}^{-3}$  wet resin) is the concentration of phosphate on the functional groups, in equilibrium with the concentration of phosphate in the bulk solution  $C_0$  ( $\text{mol m}^{-3}$ ). The first and second terms of the right-hand side of Eq. 2 show the contributions of pore diffusion and surface diffusion, respectively. In this parallel diffusion model,  $\alpha$  and  $\beta$  are the most important parameters. According to the definition of  $\alpha$ , it means a distribution coefficient.  $\beta$  can be rewritten as follows

$$\beta = \alpha \frac{D_s}{D_p} = \left( q_0 \frac{15D_s}{r_0^2} \right) / \left( \varepsilon_p C_0 \frac{15D_p}{r_0^2} \right) = \frac{k_s q_0}{k_p \varepsilon_p C_0} \quad (3)$$

where  $k_s (=15D_s/r_0^2)$  and  $k_p (=15D_p/r_0^2)$  are the intraparticle mass transfer coefficients based on surface and pore diffusions, respectively. Equation 3 shows that  $\beta$  is the ratio of the rate of surface diffusion to that of pore diffusion. In other words, the degree of contributions of surface and pore diffusions should not be simply estimated from  $D_s/D_p$ , but must be evaluated from the value of  $\beta$ . There are two limiting cases to consider here: when  $\beta = 0$  ( $k_s q_0 = 0$ ; pore diffusion control) and when  $\beta = \infty$  ( $k_p \varepsilon_p C_0 = 0$ ; surface diffusion control). When  $\beta = 0$ , the second term of the righthand side of Eq. 2 becomes zero and the equation for the pore diffusion control is obtained. However, when  $\beta = \infty$ , the second term of Eq. 2 becomes infinite and, consequently, the equation cannot be solved directly. Therefore, Eq. 1 is transformed into the following equation

$$\frac{\partial X}{\partial \tau_s} + \alpha \frac{\partial Y}{\partial \tau_s} = \frac{\alpha}{\rho^2} \frac{\partial}{\partial \rho} \left( \rho^2 \frac{\partial Y}{\partial \rho} \right) \quad (\text{surface diffusion control, } \beta = \infty) \quad (4)$$

where  $\tau_s = D_s t / r_0^2$ .

Applying the Langmuir isotherm expressed by Eq. 5 and using assumption 4, Eqs. 2 and 4 are transformed into Eqs. 6 and 7, respectively, as follows

$$Y = \frac{X}{R + (1 - R)X} \quad (5)$$

$$\left[ \alpha + \frac{R}{\{1 - (1 - R)Y\}^2} \right] \frac{\partial Y}{\partial \tau_p} = \frac{1}{\rho^2} \frac{\partial}{\partial \rho} \left[ \rho^2 \frac{R}{\{1 - (1 - R)Y\}^2} \frac{\partial Y}{\partial \rho} \right] + \frac{\beta}{\rho^2} \frac{\partial}{\partial \rho} \left( \rho^2 \frac{\partial Y}{\partial \rho} \right) \quad (6)$$

$$\left[ \alpha + \frac{R}{\{1 - (1 - R)Y\}^2} \right] \frac{\partial Y}{\partial \tau_s} = \frac{\alpha}{\rho^2} \frac{\partial}{\partial \rho} \left( \rho^2 \frac{\partial Y}{\partial \rho} \right) \quad (\text{surface diffusion control, } \beta = \infty) \quad (7)$$

As mentioned previously, Eq. 6 includes the expression of the pore diffusion control ( $\beta = 0$ ). The initial and boundary conditions are given by the following equation

$$\left. \begin{array}{l} \text{(I.C.) } X = 0 \quad Y = 0 \quad \text{at } \tau_p = 0 \quad \text{or } \tau_s = 0 \\ \text{(B.C.) } \frac{\partial X}{\partial \rho} = 0 \quad \frac{\partial Y}{\partial \rho} = 0 \quad \text{at } \rho = 0 \\ X = 1 \quad Y = 1 \quad \text{at } \rho = 1 \end{array} \right\} \quad (8)$$

Given that, experimentally, only the change in the total concentration of phosphate ions in the particle  $Q$  (mol m<sup>-3</sup> wet resin) in Eq. 9 can be determined with time, then the fractional attainment of equilibrium  $F$  is defined by Eq. 10, as follows

$$Q = q + \varepsilon_p C \quad (9)$$

$$F = \frac{\bar{Q}}{Q_0} = \frac{3 \int_0^{r_0} Q r^2 dr}{r_0^3 Q_0} = \frac{3 \left[ \alpha \int_0^1 Y \rho^2 d\rho + \int_0^1 X \rho^2 d\rho \right]}{\alpha + 1} \quad (10)$$

where  $Q_0 = q_0 + \varepsilon_p C_0$ . Apparently, Eqs. 6 and 7 are both nonlinear differential equations. To obtain their respective numerical solutions, these two equations are first transformed into finite differential equations. Then the solutions for the change in  $F$  with time are obtained.

When  $\alpha (=q_0/\varepsilon_p C_0) = \infty$ , the concentration of phosphate on the functional groups is substantially larger than that in the pore. In this case, pore diffusion is negligible and the surface diffusion is the rate-controlling step. This is confirmed by substituting  $\alpha = \infty$  into Eq. 2. Dividing both sides of Eq. 2 by  $\alpha$  and using the definition of  $\beta [= \alpha(D_s/D_p)]$ , the terms related to the concentration of phosphate in the pore disappear and the following equation is obtained

$$\frac{\partial Y}{\partial \tau_s} = \frac{1}{\rho^2} \frac{\partial}{\partial \rho} \left( \rho^2 \frac{\partial Y}{\partial \rho} \right) \quad (\text{surface diffusion control, } \alpha = \infty) \quad (11)$$

Moreover, when  $\alpha = \infty$ , Eq. 10 is also reduced to Eq. 12, as follows

$$F = \frac{3 \int_0^{r_0} Q r^2 dr}{r_0^3 Q_0} = 3 \int_0^1 Y \rho^2 d\rho \quad (12)$$

Equation 11 has been normally used as a basic equation for the surface diffusion model. Finally, the solution to the equation for the fractional attainment of equilibrium under the initial and boundary conditions in Eq. 8 is given by Eq. 13 (Carslaw and Jaeger, 1959)

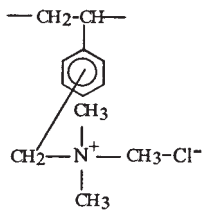
$$F = \frac{\bar{Q}}{Q_0} = \frac{3 \int_0^{r_0} Q r^2 dr}{r_0^3 Q_0} = 1 - \frac{6}{\pi^2} \sum_{n=1}^{\infty} \frac{1}{n^2} \exp \left( - \frac{D_{eff} n^2 \pi^2 t}{r_0^2} \right) \quad (13)$$

This is to emphasize that Eq. 11 can be used only when  $\alpha = \infty$ . When  $\alpha$  is relatively large but not infinite, the surface diffusion control expressed by Eq. 11 can be used only when  $\beta \gg 1$ . Otherwise, even if  $\alpha$  is large, Eq. 6 must be solved. These cases are discussed in greater detail in the Results and Discussion section.

## Experimental Studies

The phosphate compounds H<sub>3</sub>PO<sub>4</sub> and Na<sub>3</sub>PO<sub>4</sub>·12H<sub>2</sub>O were purchased from Nacalai Tesque Inc. (Kyoto, Japan), and the compounds NaH<sub>2</sub>PO<sub>4</sub>·2H<sub>2</sub>O and Na<sub>2</sub>HPO<sub>4</sub>·12H<sub>2</sub>O were ob-

**Table 1. Experimental Physical Properties of DIAION SA10A**

Unit molecular structure		
Particle size range (dry state)	US standard mesh	24–28
Particle diameter		
dry, OH <sup>−</sup> type*	meter	$6.756 \times 10^{-4}$
wet, OH <sup>−</sup> type*	meter	$8.223 \times 10^{-4}$
wet, H <sub>3</sub> PO <sub>4</sub> type**	meter	$7.778 \times 10^{-4}$
wet, H <sub>2</sub> PO <sub>4</sub> <sup>−</sup> type**	meter	$7.922 \times 10^{-4}$
wet, HPO <sub>4</sub> <sup>2−</sup> type**	meter	$8.016 \times 10^{-4}$
wet, PO <sub>4</sub> <sup>3−</sup> type**	meter	$8.198 \times 10^{-4}$
True density	kg of dry resin m <sup>−3</sup>	1.131
Apparent density	kg of wet resin m <sup>−3</sup>	0.685
Porosity	[—]	0.393

\*Average of 50 particles.

\*\*Average of 10 particles.

tained from Kishida Chemical Co. (Osaka, Japan). The phosphate compounds and other chemicals used were all special grade and used as received.

The commercially available strongly basic ion exchanger, DIAION SA10A, was purchased from Mitsubishi Chemical Co. (Tokyo, Japan). The polymer network is made of styrene-divinylbenzene, and its functional group is a quaternary ammonium (type I). The experimental physical properties of DIAION SA10A are listed in Table 1. The procedures on the characterization and conditioning of the resin, and the details on feed concentration determination, are all well discussed in the literature (Yoshida and Galinada, 2002). The experimental systems and conditions for the uptake study are summarized in Table 2.

The uptake curves for adsorption of phosphate ions on DIAION SA10A were measured by the shallow-bed method. Figure 1 shows the experimental setup used for the shallow-bed method. The detachable shallow-bed column ⑥ was prepared using the following procedures. A glass tube with an inside diameter of  $1.5 \times 10^{-2}$  m was cut to a column length of  $5.0 \times 10^{-2}$  m. The glass column was then carefully inserted into a PVC tube. After insertion, both ends of the plastic tube were cut at a length  $1.0 \times 10^{-2}$  m longer than the total length of the glass column, to be able to fit, connect, and reconnect the column into the overall shallow-bed experimental apparatus. Finally, a plastic net with a mesh size smaller than the resin particle diameter was cut to a round shape that is equal to the outside diameter of the glass column. Two nets were prepared for both ends of the column. These nets are removable and they

prevent the resin particles from flowing out of the shallow-bed column.

For every uptake measurement, a fixed amount ( $1.0 \times 10^{-4}$  kg) of resin particles was placed inside the column, which gave a resin bed thickness of one or two particle layers (about  $1.5\text{--}2.0 \times 10^{-3}$  m) inside the shallow-bed column. The resin bed was sufficiently thin to prevent any change in the bulk solution concentration of phosphates during the adsorption process. The void fraction of the shallow-bed column was not particularly taken into consideration because the column was not entirely filled with resin particles; thus they are all free to move inside the shallow-bed column during the adsorption process. The amount of the bulk solution was sufficiently large to keep the phosphate concentration essentially constant throughout the uptake measurements. The phosphate solution was allowed to flow through the shallow-bed column ⑥ from the feed tank ① (see Figure 1) at various periods of contact time. The solution was fed at a high speed ( $Re_p \approx 3250$ ) to neglect liquid film diffusion resistance surrounding the particles. After each contact time, the solution inside the column was immediately removed using a vacuum aspirator for about 1 to 2 s (B-direction) and then the solution surrounding the resin particles was instantaneously washed with ultrapure water for about 4 to 5 s (C-direction). Thereafter, the resin particles were removed from the column and placed inside a  $1.0 \times 10^{-4}$ -m<sup>3</sup> flask in which  $5.0 \times 10^{-5}$  m<sup>3</sup> of 2 kmol m<sup>−3</sup> of NaOH aqueous solution was added for the desorption process. The phosphates in the resin phase were completely desorbed after 4 days. The phosphate concentration in the eluate was determined by high-performance liquid chromatography (HPLC-LC-10A, Shimadzu, Kyoto, Japan). The resin-phase concentration of phosphates  $q$  (mol m<sup>−3</sup> wet resin) was calculated according to Eq. 14 as follows

$$q = \frac{C_e V_e \rho}{W} \quad (14)$$

where  $C_e$  (mol m<sup>−3</sup>) is the concentration of phosphate ion in the eluate;  $V_e$  (m<sup>3</sup>) is the volume of the eluate;  $\rho$  (kg m<sup>−3</sup> wet resin) and  $W$  (kg wet resin) are the apparent density and weight of the resin particles, respectively. All experiments were carried out at 298 K.

## Results and Discussion

Figures 2–5 show the experimental uptake curves for adsorption of H<sub>3</sub>PO<sub>4</sub>, H<sub>2</sub>PO<sub>4</sub><sup>−</sup>, HPO<sub>4</sub><sup>2−</sup>, and PO<sub>4</sub><sup>3−</sup> ions in OH-type strongly basic ion exchanger, DIAION SA10A, for the whole range of phosphate concentrations considered. It is clear that the uptake rate of phosphates increased with the increase in the bulk phase concentration of phosphates. The solid lines are all theoretical lines obtained in the following manner.

**Table 2. Experimental Systems and Conditions**

Resin	Type of Resin	Adsorbates Used <sub>(aq)</sub>	Feed Concentrations (kmol m <sup>−3</sup> )	Temperature (K)
DIAION SA10A (gel type)	OH <sup>−</sup>	H <sub>3</sub> PO <sub>4</sub>	0.10, 0.075 0.05, 0.03, 0.01	298
		NaH <sub>2</sub> PO <sub>4</sub>	0.10, 0.075 0.05, 0.03, 0.01	
		Na <sub>2</sub> HPO <sub>4</sub>	0.10, 0.075 0.05, 0.03, 0.01	
		Na <sub>3</sub> PO <sub>4</sub>	0.10, 0.075 0.05, 0.03, 0.01	

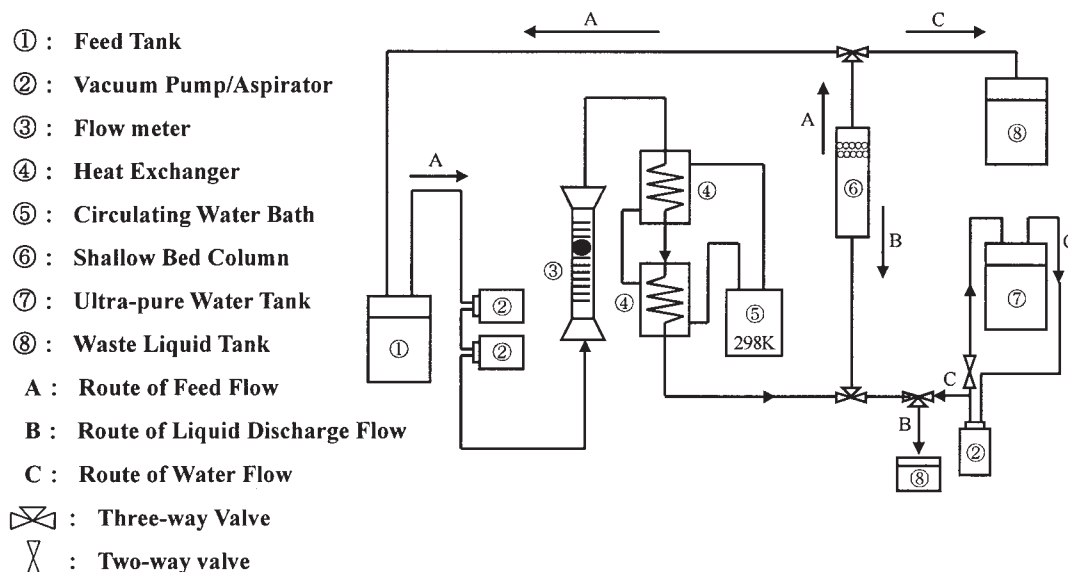


Figure 1. Experimental setup of a shallow-bed method.

### Intraparticle effective diffusivity

To determine the surface diffusivity  $D_s$  ( $\text{m}^2 \text{s}^{-1}$ ) and the pore diffusivity  $D_p$  ( $\text{m}^2 \text{s}^{-1}$ ) based on the parallel diffusion model, the intraparticle effective diffusivity  $D_{eff}$  ( $\text{m}^2 \text{s}^{-1}$ ) for the homogeneous model is calculated. Assuming Fickian diffusion with a constant intraparticle effective diffusivity, the mass balance equation over the particle is given by the following equation

$$\frac{\partial Q}{\partial t} = D_{eff} \frac{1}{r^2} \frac{\partial}{\partial r} \left( r^2 \frac{\partial Q}{\partial r} \right) \quad (15)$$

The initial (I.C.) and boundary conditions (B.C.) are given as follows

$$\left. \begin{aligned} \text{(I.C.) } Q &= 0 \quad \text{at} \quad t = 0 \\ \text{(B.C.) } \frac{\partial Q}{\partial r} &= 0 \quad \text{at} \quad r = 0 \\ Q &= Q_0 (= q_0 + \varepsilon C_0) \quad \text{at} \quad r = r_0 \end{aligned} \right\} \quad (16)$$

The fractional attainment of equilibrium is given by Eq. 17 (Carslaw and Jaeger, 1959)

$$F = \frac{3 \int_0^{r_0} Q r^2 dr}{r_0^3 Q_0} = \frac{3 \left[ \alpha \int_0^1 Y \rho^2 d\rho + \int_0^1 X \rho^2 d\rho \right]}{\alpha + 1} = 1 - \frac{6}{\pi^2} \sum_{n=1}^{\infty} \frac{1}{n^2} \exp \left( - \frac{D_{eff} n^2 \pi^2 t}{r_0^2} \right) \quad (17)$$

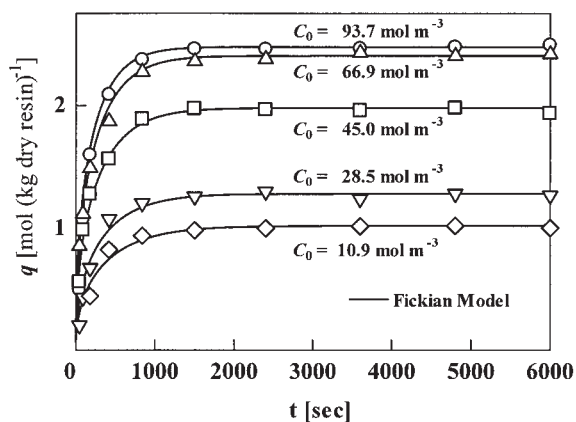


Figure 2. Effect of concentration on the uptake curves for adsorption of  $\text{H}_3\text{PO}_4$  on OH-type DIAION SA10A.

$D_{eff}$  values are listed in Table 3.

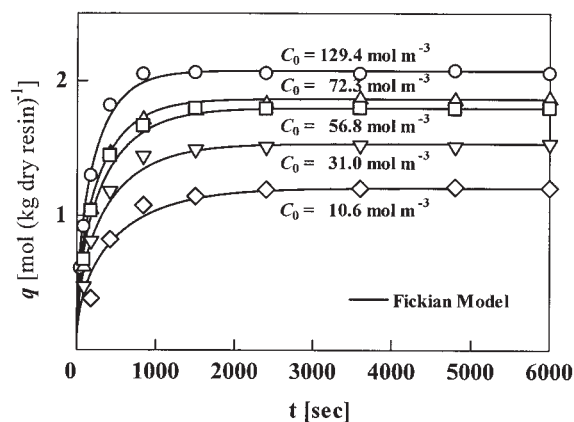
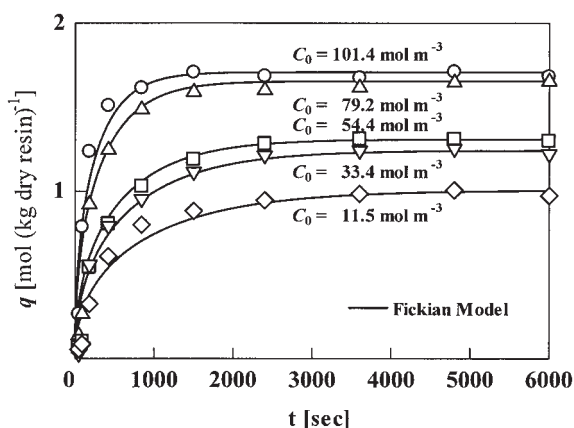


Figure 3. Effect of concentration on the uptake curves for adsorption of  $\text{NaH}_2\text{PO}_4$  on OH-type DIAION SA10A.

$D_{eff}$  values are listed in Table 3.



**Figure 4. Effect of concentration on the uptake curves for adsorption of  $\text{Na}_2\text{HPO}_4$  on OH-type DIAION SA10A.**

$D_{\text{eff}}$  values are listed in Table 3.

The values of the intraparticle effective diffusivity ( $D_{\text{eff}}$ ) were determined by fitting the experimental uptake data with Eq. 17, initializing different values of  $D_{\text{eff}}$  until the best fit was obtained. As shown in Figures 2–5, the experimental values were all well correlated by Eq. 17. The experimental values of  $D_{\text{eff}}$  are all listed in Table 3. For all phosphate systems,  $D_{\text{eff}}$  increased with increasing bulk-phase phosphate concentration. These suggested an existence of a parallel transport by both surface and pore diffusions in the particle. The values of  $D_{\text{eff}}$  in both  $\text{H}_3\text{PO}_4$  and  $\text{Na}_3\text{PO}_4$  systems are larger than those for  $\text{NaH}_2\text{PO}_4$  and  $\text{Na}_2\text{HPO}_4$  systems. This result also conforms to the order of  $D_{\text{eff}}$  values obtained in our breakthrough experiments (results will soon be published separately).

#### Surface diffusivity and approximate pore diffusivity

The relation between surface diffusivity, pore diffusivity, and intraparticle effective diffusivity based on parallel diffusion model is given by the following equation (Yoshida et al., 1994)

$$D_{\text{eff}} \left( 1 + \varepsilon \frac{dC}{dq} \right) = D_s + \varepsilon D_p \frac{dC}{dq} \quad (18)$$

In this particular study, because the experimental adsorption isotherms were not linear,  $dC/dq$  was not simply determined from the equilibrium isotherm. However, by taking an approximation that  $dC/dq = C_0/q_0$ , as expressed by Eq. 19, Eq. 18 is then transformed into Eq. 20 (Yoshida et al., 1994), as follows

$$\frac{1}{q_0} \int_0^{q_0} \frac{dC}{dq} dq = \frac{C_0}{q_0} \quad (19)$$

$$D_{\text{eff}} \left( 1 + \frac{1}{\alpha} \right) = D_s + D_{pa} \frac{1}{\alpha} \quad (20)$$

where  $D_{\text{eff}}$ ,  $D_s$ ,  $D_{pa}$ , and  $\alpha (=q_0/\varepsilon_P C_0)$  are the intraparticle effective diffusivity ( $\text{m}^2 \text{s}^{-1}$ ), the surface diffusivity ( $\text{m}^2 \text{s}^{-1}$ ),

the approximate pore diffusivity ( $\text{m}^2 \text{s}^{-1}$ ), and the distribution coefficient, respectively. The approximation in Eq. 20 is correct for a linear isotherm system; however, even in a nonlinear isotherm system, the approximation will give an integral mean value of  $dC/dq$  from  $q = 0$  to  $q_0$  ( $C = 0$  to  $C_0$ ). When  $1/\alpha (= \varepsilon_P C_0/q_0) \rightarrow 0$  in Eq. 20,  $D_{\text{eff}}$  approaches  $D_s$ . However, the value of the slope of the plots in the left-hand side of the equation vs.  $1/\alpha$  may not give an accurate pore diffusivity ( $D_p$ ) because of the approximation of  $dC/dq = C_0/q_0$ . Therefore, the slope is assigned as  $D_{pa}$ , which means approximate pore diffusivity. It is only in the case when the isotherm is linear that  $D_{pa} = D_p$ . If the plot based on Eq. 20 is linear but the intercept is zero ( $D_s = 0$ ), then pore diffusion is the rate-controlling step. On the other hand, if the slope of the plot is zero ( $D_{pa} = 0$ ), then surface diffusion is the rate-controlling step. Otherwise, parallel transport by surface and pore diffusions may exist.

Figure 6 shows the plots of the experimental intraparticle effective diffusivities based on Eq. 20. For all phosphate systems, the experimental values of  $D_{\text{eff}}$  were all correlated well by straight lines. Consequently, the values of surface diffusivities  $D_s$  and approximate pore diffusivities  $D_{pa}$  were determined from the intercepts and slopes of the straight lines, respectively. They are all listed in Table 3. The experimental surface diffusivity  $D_s$  values obtained in both  $\text{H}_3\text{PO}_4$  and  $\text{NaH}_2\text{PO}_4$  systems are five to seven times larger than those in  $\text{Na}_3\text{PO}_4$  and  $\text{Na}_2\text{HPO}_4$  systems. This may be because the larger the ionic valence of the anion is, the stronger the force between the anion and the cationic fixed group becomes. Therefore, the resistance to hop from one fixed group to the next fixed group becomes greater when ionic valence increases. On the other hand, the approximate pore diffusivity  $D_{pa}$  values in the  $\text{NaH}_2\text{PO}_4$  system is about two to three times smaller than those in  $\text{Na}_3\text{PO}_4$ ,  $\text{Na}_2\text{HPO}_4$ , and  $\text{H}_3\text{PO}_4$  systems.

#### Accurate pore diffusivity

To obtain the values for the accurate pore diffusivity ( $D_p$ ), the experimental uptake data were matched with theoretical lines calculated by Eq. 6 as well as the experimental values of  $D_s$  determined earlier. Figure 7 shows the plots of  $D_p$  against  $C_0$ . In all phosphate systems, the values of  $D_p$  did not vary in

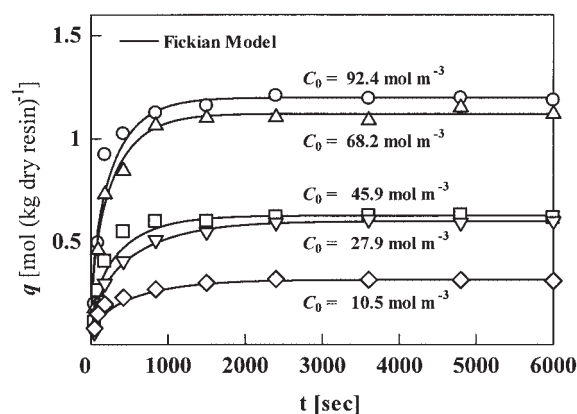


**Figure 5. Effect of concentration on the uptake curves for adsorption of  $\text{Na}_3\text{PO}_4$  on OH-type DIAION SA10A.**

$D_{\text{eff}}$  values are listed in Table 3.

Table 3. Feed Concentration against Determined Parameters

System	$C_0$ (mol m <sup>-3</sup> )	$D_{eff} \times 10^{-11}$ (m <sup>2</sup> s <sup>-1</sup> )	$D_S \times 10^{-12}$ (m <sup>2</sup> s <sup>-1</sup> )	$D_{Pa} \times 10^{-10}$ (m <sup>2</sup> s <sup>-1</sup> )	$D_{Pm} \times 10^{-10}$ (m <sup>2</sup> s <sup>-1</sup> )	$D_L \times 10^{-9}$ (m <sup>2</sup> s <sup>-1</sup> )	$D_L/D_{Pm}$ (—)	$\alpha$ (—)	$\beta$ (—)
H <sub>3</sub> PO <sub>4</sub>	93.7	5.5	21.07	16.32	4.94	1.201	2.431	38.92	1.66
	66.9	4.7						46.66	1.99
	45.0	4.4						58.21	2.48
	28.5	3.8						88.24	3.76
	10.9	3.3						114.84	4.90
H <sub>2</sub> PO <sub>4</sub> <sup>-</sup>	129.4	4.6	21.83	6.85	3.77	1.234	3.274	25.75	1.49
	72.3	3.8						43.24	2.50
	56.8	3.4						53.02	3.07
	31.0	3.0						85.02	4.92
	10.6	2.5						162.67	9.42
HPO <sub>4</sub> <sup>2-</sup>	101.4	4.9	3.98	12.12	5.89	1.271	2.157	27.16	0.18
	79.2	4.0						33.54	0.23
	54.4	2.9						45.41	0.31
	33.4	2.2						64.79	0.44
	11.5	1.6						117.34	0.79
PO <sub>4</sub> <sup>3-</sup>	92.4	5.2	3.09	12.45	5.96	1.391	2.333	23.56	0.12
	68.2	4.5						27.94	0.14
	45.9	3.9						33.73	0.17
	27.9	3.1						40.48	0.21
	10.5	2.7						50.18	0.26

the whole range of phosphate concentrations considered. The arithmetic mean values ( $D_{Pm}$ ) of  $D_p$  were then calculated and the values are listed in Table 3. The values of  $D_p$  were relatively close to the calculated values of  $D_{Pm}$  (average standard deviation = 0.1018). The values for the tortuosity factor,  $\tau_p$ , of the individual phosphate species were determined from the ratio between the liquid-phase diffusivity  $D_L$  and  $D_{Pm}$ , and they are given in Table 3. The liquid-phase diffusivities were calculated using the Wilke–Chang equation (Wilke and Chang, 1955). It must be emphasized that the values of  $\tau_p$  for all phosphate species are close to the values of about 2.2–3.3, which are normal in porous materials.

#### Parallel transport by surface and pore diffusion

For all phosphate systems, the theoretical uptake curves for adsorption of phosphates in DIAION SA10A were calculated based on the parallel transport by surface and pore diffusions, given in Eq. 6, using the experimental values of surface diffusivity ( $D_S$ ) and pore diffusivity ( $D_{Pm}$ ) in Table 3. The dimen-

sionless parameters used in the theoretical calculations are also given in Table 3.

Figures 8–11 show the experimental and theoretical uptake curves for adsorption of H<sub>3</sub>PO<sub>4</sub>, NaH<sub>2</sub>PO<sub>4</sub>, Na<sub>2</sub>HPO<sub>4</sub>, and Na<sub>3</sub>PO<sub>4</sub> in OH-type DIAION SA10A for the two of the five phosphate concentrations considered, respectively. The solid lines are the theoretical ones determined from Eq. 6. They all correlated reasonably well with the experimental uptake data. The theoretical lines for the pore diffusion control and the surface diffusion control were likewise calculated, represented by broken and chain lines, respectively. The theoretical lines for the pore diffusion control were obtained by setting the  $\beta = 0$  ( $D_S = 0$ ) in Eq. 6 and using the experimental values of  $D_{Pm}$  in Table 3. Again, when  $1/\alpha (= \varepsilon_p C_0/q_0)$  approaches zero ( $\alpha \rightarrow \infty$ ) (see Eq. 20 and Figure 6), surface diffusion is the rate-controlling step. The theoretical lines for the surface diffusion control were determined based on Eq. 11 and using the experimental values of  $D_S$  in Table 3.

In both Figures 8 and 9 (H<sub>3</sub>PO<sub>4</sub> and NaH<sub>2</sub>PO<sub>4</sub> systems), the deviation of the uptake data from the surface diffusion model

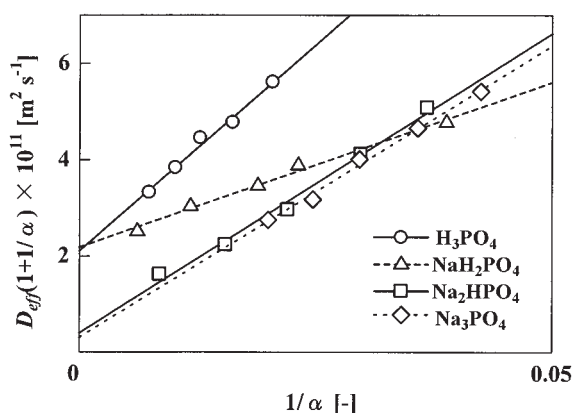


Figure 6. Plots of intraparticle effective diffusivities based on Eq. 20.

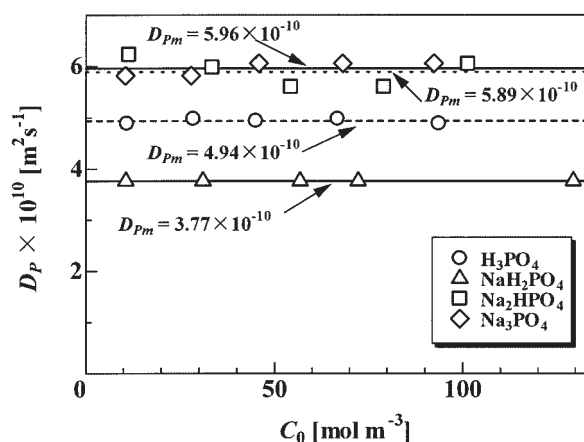


Figure 7. Plots of  $D_p$  against  $C_0$ .

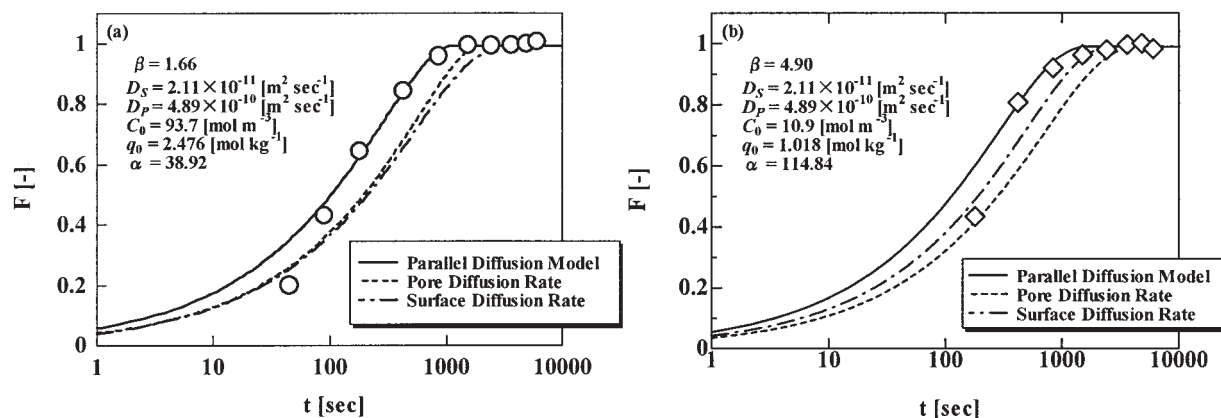


Figure 8. Experimental and theoretical uptake curves for adsorption of  $\text{H}_3\text{PO}_4$  on OH-type DIAION SA10A for  $C_0 = 93.7$  and  $C_0 = 10.9$   $[\text{mol m}^{-3}]$ .

(chain line) increased with the increase in the bulk phase concentration  $C_0$  (that is,  $\alpha$  and  $\beta$  decrease) but the deviation of the pore diffusion model (broken line) from the uptake data increased with decreasing  $C_0$ . In these two phosphate systems, at  $C_0 = 10.6 \text{ mol m}^{-3}$  with  $\beta = 9.42$ , the uptake data significantly deviated from the pore diffusion model and the adsorption rate is controlled by surface diffusion. On the other hand, when  $\beta < 0.31$  in  $\text{Na}_2\text{HPO}_4$  system (Figure 10), the uptake data are very close to the theoretical lines of the pore diffusion model (broken line) and significantly deviated from the theoretical lines of the surface diffusion model (chain line). In Figure 11 ( $\text{Na}_3\text{PO}_4$  system), all values of  $\beta$  are smaller than 0.3 and the uptake data coincided with the theoretical lines of the pore diffusion model but deviated significantly from the surface diffusion model in the whole range of phosphate concentrations considered. It is very clear that only the contribution of pore diffusion is very significant in this particular phosphate system.

As mentioned earlier in the theoretical section, there are two limiting cases to consider:  $\beta = 0$  (pore diffusion control) and  $\beta = \infty$  (surface diffusion control). From Figures 8–11, and Table 3, when  $\beta > 9$ , it is apparent that surface diffusion is the rate-controlling step. When  $\beta < 0.30$ , it can be assumed that pore diffusion is the rate-controlling step; and when  $0.30 <$

$\beta < 9$ , the parallel transport by surface and pore diffusions should be considered. These results are consistent with the study, conducted by Yoshida et al. (1994), on the parallel transport of BSA by surface and pore diffusions in two different strongly basic, highly porous chitosan beads.

The values of  $D_S$  of  $\text{H}_2\text{PO}_4^-$  and  $\text{H}_3\text{PO}_4$  in Table 3 are about five to seven times larger than those of  $\text{HPO}_4^{2-}$  and  $\text{PO}_4^{3-}$ . These may be caused by the weaker affinity between the fixed cation group and the adsorbates  $\text{H}_2\text{PO}_4^-$  and  $\text{H}_3\text{PO}_4$  than that in  $\text{HPO}_4^{2-}$  and  $\text{PO}_4^{3-}$ . Given that  $\text{HPO}_4^{2-}$  and  $\text{PO}_4^{3-}$  ions have larger ionic valences than those of the  $\text{H}_2\text{PO}_4^-$  ion, then they are more strongly anchored on the fixed groups, occupying two and three fixed groups at the same time, respectively. Thus, hopping of  $\text{HPO}_4^{2-}$  and  $\text{PO}_4^{3-}$  ions from one site to the next nearest available site is very slow and, consequently, allows the  $\text{H}_2\text{PO}_4^-$  ion to occupy more fixed-functional groups in the resin.

## Conclusions

The intraparticle mass transport of  $\text{H}_3\text{PO}_4$ ,  $\text{H}_2\text{PO}_4^-$ ,  $\text{HPO}_4^{2-}$ , and  $\text{PO}_4^{3-}$  ions in an OH-type strongly basic ion exchanger, DIAION SA10A, was investigated. The values of the intraparticle effective diffusivity ( $D_{\text{eff}}$ ) obtained from the homogeneous Fickian model increased with increasing bulk-phase concentra-

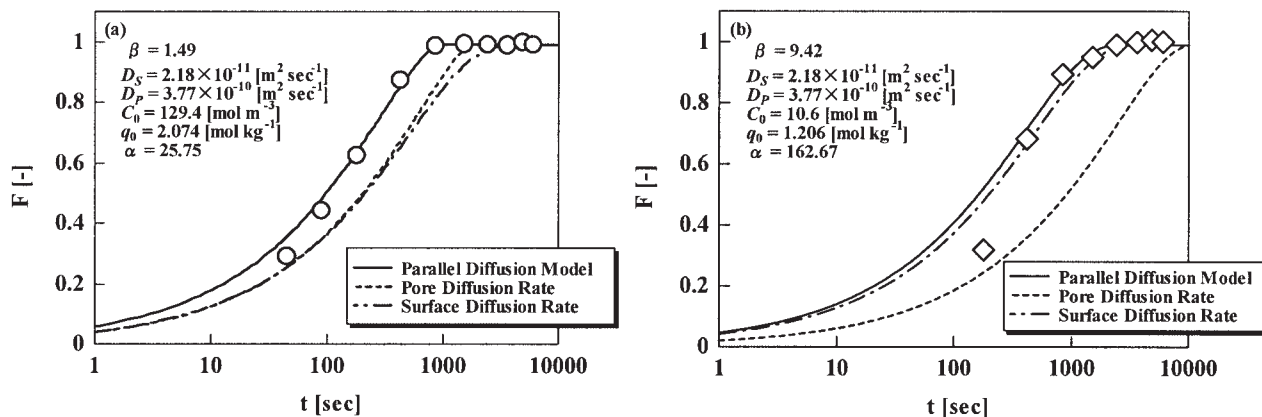


Figure 9. Experimental and theoretical uptake curves for adsorption of  $\text{NaH}_2\text{PO}_4$  on OH-type DIAION SA10A for  $C_0 = 129.4$  and  $C_0 = 10.6$   $[\text{mol m}^{-3}]$ .

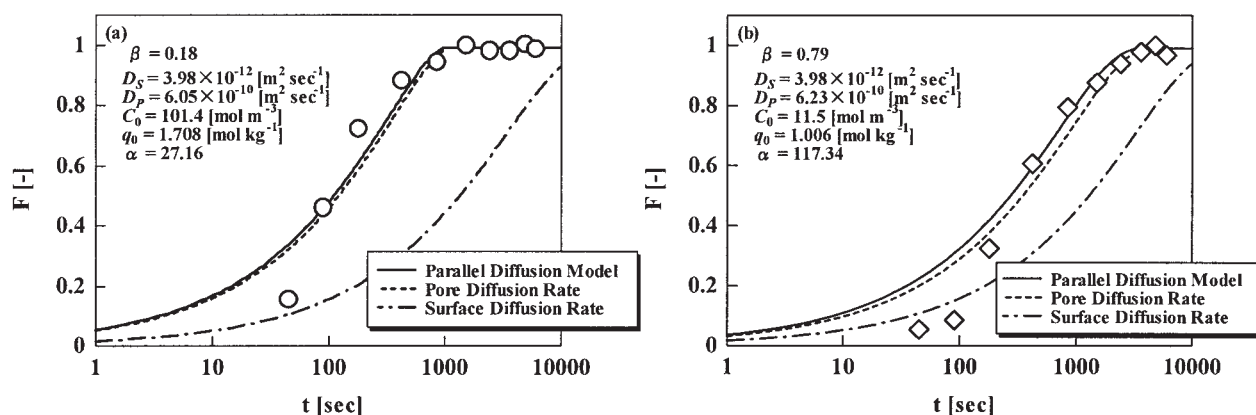


Figure 10. Experimental and theoretical uptake curves for adsorption of  $\text{Na}_2\text{HPO}_4$  on OH-type DIAION SA10A for  $C_0 = 101.4$  and  $C_0 = 11.5$  [ $\text{mol m}^{-3}$ ].

tion for the whole range of phosphate concentrations considered. The surface diffusivities ( $D_S$ ) for the parallel diffusion model were determined from the intercepts of the plots of  $D_{\text{eff}}[1 + (\varepsilon_P C_0/q_0)]$  vs.  $\varepsilon_P C_0/q_0$ . The experimental surface diffusivity  $D_S$  values of  $\text{H}_2\text{PO}_4^-$ , obtained in both  $\text{H}_3\text{PO}_4$  and  $\text{NaH}_2\text{PO}_4$  systems, were five to seven times larger than those in  $\text{PO}_4^{3-}$  and  $\text{HPO}_4^{2-}$ . These may be caused by the weaker affinity between the fixed cationic group and the adsorbate  $\text{H}_2\text{PO}_4^-$  than that in  $\text{HPO}_4^{2-}$  and  $\text{PO}_4^{3-}$ . In all phosphate systems, the values of  $D_P$  did not vary in the whole range of phosphate concentrations considered. The ratios of  $D_L/D_{Pm}$  were not dependent on the ionic species of phosphates and the obtained values 2.2–3.3 are normal values in porous materials. The theoretical lines of the parallel diffusion model using  $D_S$  and  $D_{Pm}$  agreed reasonably well with the experimental uptake data. Surface diffusion is the rate-controlling step when  $\beta > 9$ , whereas pore diffusion is the rate-controlling step when  $\beta < 0.30$ . When  $0.30 < \beta < 9$ , the parallel transport by surface and pore diffusions should be considered.

## Acknowledgments

This research was partly supported by the Ministry of Education, Culture, Sports, Science and Technology of Japan under the 21st Century Center of Excellence (COE-21) Program, 24403, E-1, entitled “Water-

Assisted Evolution of Valuable Resources and Energy from Organic Wastes.”

## Notation

- $C$  = liquid-phase concentration of phosphates in the pore,  $\text{mol m}^{-3}$
- $C$  = concentration of phosphate in the bulk solution,  $\text{mol m}^{-3}$
- $C_e$  = concentration of phosphate in the eluate,  $\text{mol m}^{-3}$
- $D_{\text{eff}}$  = intraparticle effective diffusivity,  $\text{m}^2 \text{s}^{-1}$
- $D_P$  = pore diffusivity based on the parallel diffusion model,  $\text{m}^2 \text{s}^{-1}$
- $D_{Pa}$  = approximate pore diffusivity determined from the slope of the plots according to Eq. 20,  $\text{m}^2 \text{s}^{-1}$
- $D_{Pm}$  = arithmetic mean pore diffusivity,  $\text{m}^2 \text{s}^{-1}$
- $D_S$  = solid-phase diffusivity based on the parallel diffusion model,  $\text{m}^2 \text{s}^{-1}$
- $F$  = fractional attainment of equilibrium
- $k_S$  =  $(=15D_S/r_0^2)$  intraparticle mass transfer coefficient based on solid-phase diffusion,  $\text{s}^{-1}$
- $k_P$  =  $(=15D_P/r_0^2)$  intraparticle mass transfer coefficient based on pore diffusion,  $\text{s}^{-1}$
- $q$  = resin-phase concentration of phosphates on the solid-phase of the pore wall,  $\text{mol m}^{-3}$  wet resin
- $q$  = resin-phase concentration of phosphates in equilibrium with  $C_0$ ,  $\text{mol m}^{-3}$  wet resin
- $r$  = radial dimension of adsorbent particle,  $\text{m}$
- $r$  = radius of adsorbent particle,  $\text{m}$
- $Q$  =  $(=q + \varepsilon_P C_0)$  total concentration of phosphates in the particle,  $\text{mol m}^{-3}$  wet resin
- $Q$  =  $(=q_0 + \varepsilon_P C_0)$   $\text{mol m}^{-3}$  wet resin

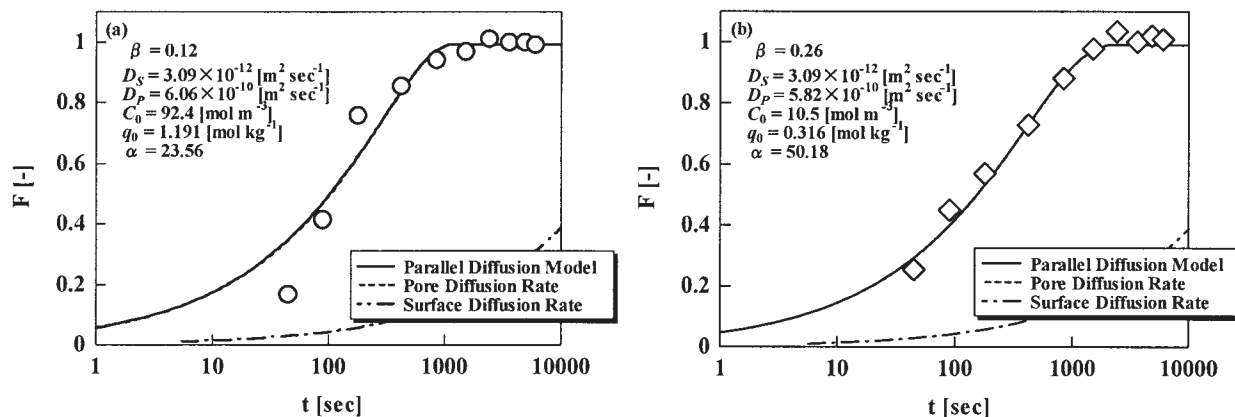


Figure 11. Experimental and theoretical uptake curves for adsorption of  $\text{Na}_3\text{PO}_4$  on OH-type DIAION SA10A for  $C_0 = 92.4$  and  $C_0 = 20.5$  [ $\text{mol m}^{-3}$ ].

$R$  = dimensionless Langmuir equilibrium constant  
 $t$  = time, s  
 $V_e$  = volume of the eluate, m<sup>3</sup>  
 $W$  = weight of resin particles, kg  
 $X$  = ( $=C/C_0$ ) dimensionless constant  
 $Y$  = ( $=q/q_0$ ) dimensionless constant

## Greek letters

$\alpha = q_0/\varepsilon C_0$   
 $\beta = \alpha(D_s/D_p) = k_s q_0/k_p \varepsilon C_0$   
 $\varepsilon_p$  = porosity of the resin particle  
 $r = r/r_0$   
 $\tau_p$  = tortuosity factor  
 $\tau_p = D_p t/r_0^2$   
 $\tau_s = D_s t/r_0^2$

## Literature Cited

- Bhandari, V. M., V. A. Juvekar, and S. R. Patwardhan, "Sorption Studies on Ion Exchange Resins. 1. Sorption of Strong Acids on Weak Base Resins," *Ind. Eng. Chem. Res.*, **31**(4), 1063 (1992a).
- Bhandari, V. M., V. A. Juvekar, and S. R. Patwardhan, "Sorption Studies on Ion Exchange Resins. 2. Sorption of Weak Acids on Weak Base Resins," *Ind. Eng. Chem. Res.*, **31**(4), 1073 (1992b).
- Bhandari, V. M., V. A. Juvekar, and S. R. Patwardhan, "Sorption of Dibasic Acids on Weak Base Resins," *Ind. Eng. Chem. Res.*, **32**(1), 200 (1993).
- Bhandari, V. M., V. A. Juvekar, and S. R. Patwardhan, "Ion Exchange Studies in the Removal of Polybasic Acids. Anomalous Sorption Behavior of Phosphoric Acid on Weak Base Resins," *Sep. Sci. Technol.*, **32**(15), 2481 (1997).
- Carlslaw, H. S., and J. C. Jaeger, *Conduction of Heat in Solids*, Oxford Univ. Press, London (1959).
- Gutsche, R., and H. Yoshida, "Solid Diffusion in the Pores of Cellulose Membrane," *Chem. Eng. Sci.*, **49**(2), 179 (1994).
- Helfferich, F. G., and Y. L. Hwang, "Kinetics of Acid Uptake by Weak-Base Anion Exchangers. Mechanism of Proton Transfer," *Ads. & Ion Exch. in AIChE Symp. Ser.*, **81**(242), 17 (1985).
- Kataoka, T., H. Yoshida, and Y. Ozasa, "Intraparticle Ion Exchange Mass Transfer Accompanied by Instantaneous Irreversible Reaction," *Chem. Eng. Sci.*, **32**, 1237 (1977).
- Maekawa, M., M. Udaka, M. Sasaki, Y. Tsujii, H. Yoshida, T. Kataoka, and M. Nango, "Diffusion Mechanism of Direct Dyes into a Cellulose Membrane: The Structural Effect of Direct Dyes on the Adsorption Rate," *J. Appl. Polym. Sci.*, **37**, 2141 (1989).
- Nango, M., Maekawa, M. Tsujii, Y. Yoshida, H. and Kataoka, T. "Transport of Various Direct Dyes into Cellulose Membrane in the Presence of Polyelectrolyte," *Transaction*, **45**(4), 159 (1989).
- Rao, M. G., and A. K. Gupta, "Kinetics of Ion-Exchange in Weak-Base Anion Exchange Resins," *Ads. & Ion Exch. in AIChE Symp. Ser.*, **78**(219), 96 (1982).
- Takatsuji, W., and H. Yoshida, "Parallel Transport by Surface and Macropore Diffusion in a Polyaminated Highly Porous Chitosan Bead in Case of Acetic Acid and Lactic Acid," *J. Chem. Eng. Jpn.*, **34**(1), 55 (2001).
- Wilke, C. R., and P. Chang, "Correlation of Coefficient in Dilute Solutions," *AIChE J.*, **1**, 264 (1955).
- Yoshida, H., and W. A. Galinada, "Equilibria for Adsorption of Phosphates on OH-Type Strongly Basic Ion Exchanger," *AIChE J.*, **48**(10), 2192 (2002).
- Yoshida, H., and T. Kataoka, "Intraparticle Mass Transfer in Bidispersed Porous Ion Exchanger. Part II: Mutual Ion Exchange," *Can. J. Chem. Eng.*, **63**, 430 (1985).
- Yoshida, H., T. Kataoka, and S. Ikeda, "Intraparticle Mass Transfer in Bidispersed Porous Ion Exchanger. Part I: Isotopic Ion Exchange," *Can. J. Chem. Eng.*, **63**, 422 (1985).
- Yoshida, H., T. Kataoka, M. Maekawa, and Nango, M. "Surface Diffusion of Direct Dyes in Porous Membranes," *Chem. Eng. J.*, **41**, B1 (1989).
- Yoshida, H., T. Kataoka, M. Nango, S. Ohta, N. Kuroki, and M. Maekawa, "Transport of Direct Dye into Cellulose Membrane," *J. Appl. Polym. Sci.*, **32**, 4185 (1986).
- Yoshida, H., M. Maekawa, and M. Nango, "Parallel Transport by Surface and Pore Diffusion in a Porous Membrane," *Chem. Eng. Sci.*, **46**(2), 429 (1991).
- Yoshida, H., and W. Takatsuji, "Parallel Transport of an Organic Acid by Surface and Macropore Diffusion in a Weakly Basic Ion Exchanger," *Ind. Eng. Chem. Res.*, **39**(4), 1074 (2000).
- Yoshida, H., M. Yoshikawa, and T. Kataoka, "Parallel Transport of BSA by Surface and Pore Diffusion in Strongly Basic Chitosan," *AIChE J.*, **40**(12), 2034 (1994).

Manuscript received July 9, 2003, and revision received Feb. 25, 2004.